

A. Al-Ghaban 

Materials Engineering
Department, University of
Technology, Baghdad, Iraq
a.ghabban@gmail.com

Aluminum Concentration Drives the Structural Evolution of Magnetron Sputtering (Ti, Al) C Thin Film

Abstract- The effect of deposited Al on the structural evolution of TiC films with a chemical composition variation has investigated during combinatorial magnetron sputtering of binary ceramic (Ti, Al) C. The here produced thin films have been investigated by energy dispersive X-ray spectroscopy (EDX) and X-ray diffraction technique XRD. The structural evolution of combinatorial magnetron sputtered Ti-Al-C system deposited at room temperature fined to be located in the extent of: Ti at.% = 36.74-60.55, Al at.% = 12.05-30.61 and C at.% = 22.53-47.69. XRD results show that films are constituted of mostly cubic (Ti, Al) C phase as well as an X-ray amorphous region in the range of Ti at. % = 37.31-54, Al at. % = 27.67-30.61 and C at. % = 22.53-36.92. A clear evidence for the formation of two different structural regions driving by Al concentration has been observed. X ray analysis also shows that the (111) orientation in the (Ti, Al) C phase is dominant with increasing the Ti concentration.

Received on: 17/08/2017

Accepted on: 23/11/2017

Keywords- Aluminium, Magnetron Sputtering, TiCx, Structural Evolution.

How to cite this article: A. Al-Ghaban "Aluminum Concentration Drives the Structural Evolution of Magnetron Sputtering (Ti, Al) C Thin Film," *Engineering and Technology Journal*, Vol. 36, Part A, No. 1, pp. 70-74, 2018.

1.

There is an increasing interest worldwide in hard coatings, thin film applications. For example, coatings in the Ti-Al-C-N system, including the ternary (Ti, Al) N phase have many promising high temperature properties [1]. Furthermore, physical vapor deposited (Ti, Al) N and (Ti, Al) (C, N) coatings were established for tribological and some new molds and extrusion dies applications in view of the thermal and mechanical stabilities [2, 3]. With the advent of magnetron sputtering, it has expected to replace conventional coating methods and generated many new applications and markets. Based on the large increase of new industrial applications, the need of tailoring and testing new materials with high efficiency is required. The Ti-Al-C system contains many ternary phases that are needed in thin film applications [4]. For instance, the combination of superconductivity and mechanical properties of the perovskite Ti₃AlC makes it a potential candidate as a superconductor [4]. The existence of the so-called MAX phases (space group P63/mmc) pushes to make the Ti-Al-C system further motivated. Over recent years, this new family of layered ceramics has attracted much attention due to their unique combination of physical and mechanical properties combined from ceramic and metallic materials [5-9]. They exhibit the hexagonal structure as ternary compounds with the general formula of Mn+1AX_n, where n is varying from 1 to 3, M is an early transition Aluminum, A is an A-group

Introduction

(mostly IIIA and IVA, or groups 13 and 14) element and X is either carbon and/or nitrogen. MAX phases are good thermal and electrical conductors [10,11]. They are also resisting to thermal shock. Beside all they are damage tolerant [12] and corrosion /oxidation resistant [13, 14]. Among this group of materials, Ti₂AlC and Ti₃AlC₂ have been widely studied in both bulk and thin film forms. Sintering of mixture of element or some compounds is the most active way to grow MAX phases [15-19] as well as by magnetron sputtering technique of single compound or elemental targets [4, 20-23].

The Titanium-Aluminum-Carbon system includes the perovskite structure of ternary carbide of Ti₃AlC. This structure is frequently formed as precipitations in bulk form [24-26].

Most all binary phases like Titanium carbide that formed in the Titanium-Aluminum-Carbon system can give a limited solid solution behavior of the third component. However, thin-film techniques such as PVD can be run at low temperature levels where atomic mobility is slow and the diffusion boundaries are very limited. These thin layers are metastable, but could show amended properties as compared with the stable once. Hence, this can be highly motivating for many thin solid layers applications with new set of properties. For instants, the metastable phase of (Ti, Al) N is widely used in tribological coatings that may contain 60% at. Al on the metallic side. The protecting oxide layer formed

at higher temperatures may be responsible for the improved properties [27, 28]. Furthermore, Hörling et al. [29] mentioned that the thin solid films of metastable Titanium–Aluminum–Nitrogen ternary phase deposited at low temperatures could be age hardened into TiN and AlN. Hence, and due to the similarity between TiN and TiC, it is expected that (Ti, Al) C may form by sputtering and have some interesting properties. It should be noted that other attempts to study the phase evolutions in the Ti–Al–C bulk system was previously carried out [30].

Here, a clear evidence for the formation of (Ti, Al) C is found due to the results gained by XRD and EDX. X-ray analysis also shows that the (111) orientation in the (Ti, Al) C phase is dominant with increasing the Ti concentration.

2. Experimental Details

Ti–Al–C film of 1.5 μm thick was deposited combinatorially from three elemental targets in a high vacuum chamber. Three magnets are set with a tilted angle of $\sim 14^\circ$ as respect with the substrate. Fig. 1a shows the deposition of the Ti–Al–C layer. The target dimensions were $\text{Ø}39$ mm and 3 mm thickness. The chamber was pumped down to a base pressure of $\sim 10^{-4}$ Pa. Pure Titanium, pure Aluminum and pure Carbon targets were sputtered in 0.3 Pa Ar atmosphere. The power densities of 4.18 for Ti, 0.83 for Al and 6.7 W/cm² for C, were respectively set. The substrate to target distance is about 50 mm. No heater or biasing were used during deposition. Single crystal sapphire wafer (99.996%, c-plane, one side polished, and a diameter of 50.8 cm) was used as a substrate. Steel grid of 145 holes with $\text{Ø}=3.5$ mm Fig. 1b was placed on the substrate during deposition for masking purposes. After the deposition, the chemical composition and the structure of 145 positions of Ti–Al–C films were analyzed.

Chemical composition analysis of the Ti–Al–C films was performed by energy dispersive X-ray analysis (EDX) with an EDAX Genesis 2000 system using an acceleration voltage of 12 KV. Ti–Al–C sample, quantified with wavelength dispersion X-ray analysis, (WDX) used as standard. The structural analysis of the Titanium–Aluminum–Carbon films was carried out utilizing a AXS D8 discover general area detection diffraction system. The measured 2θ -range was ranged from 30° to 80° using Copper K α . The X-ray beam was collimated using a pinhole with a diameter of 0.5 mm at an incidence angle of 18° .

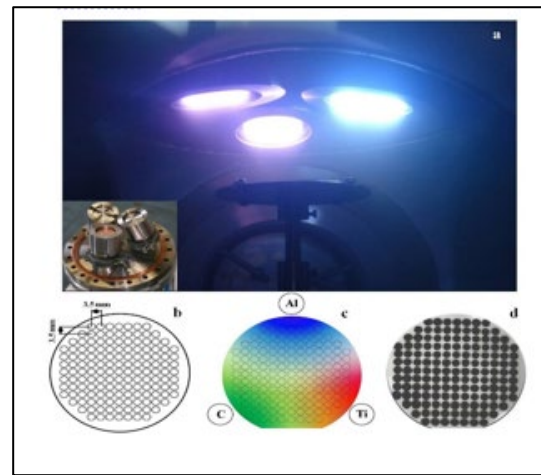


Figure 1: Deposition setup for the Ti–Al–C layer with combinatorial gradient and a drawing of the combinatorial designed targets (a). A schematic for the steel grid is given in (b). A schematic for the as-deposited sample architecture is given in (c) and (d)

3. Results and Discussion

Architecture of the as-deposited Ti–Al–C film with a composition gradient is shown in Figure 1 c, d. In that configuration, the so-called combinatorial sputtering can give long-range chemical composition variation for each element in one single deposition. Figure 2 shows the EDX measurement of two different positions of one single wafer used after depositing for several hours.

It can be seen that the Al concentration is varied from about 12.81 at. % to about 20.5 at. % for almost the same C/Ti ratios. (investigated sample contains 145 separated regions that cover a total composition spread of (Ti at. %= 36.74–60.55, Al at. %= 12.05–30.61 and C at. %= 22.53–47.69). Figure 3 shows the chemical composition analysis of the film and its location in the ternary Ti–Al–C system. The whole XRD analysis of the as-deposited films can be summarized also in Figure 3.

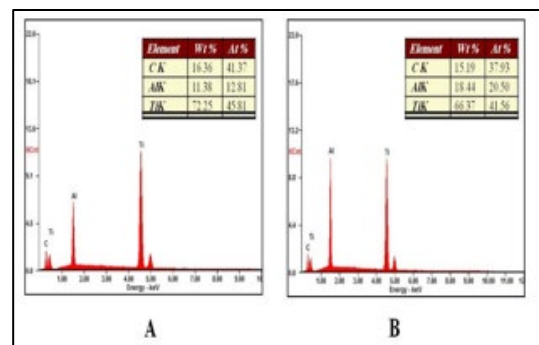


Figure 2: Plot of the chemical compositions of all deposited samples in the Ti–Al–C system together with the compositions of stoichiometric Ti₂AlC and Ti₃AlC₂ MAX phases, Ti₃AlC and TiC

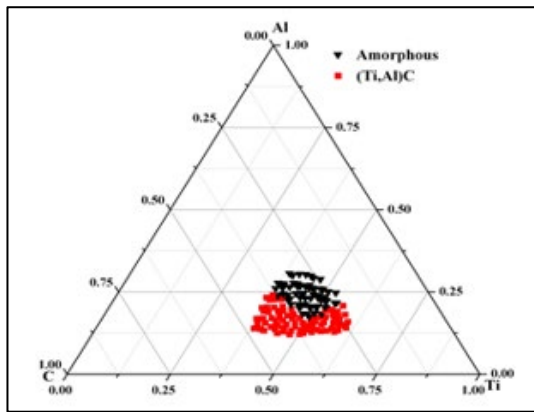


Figure 3: Plot of the chemical compositions of all deposited samples in the Ti-Al-C system represents the structural positions of both the crystalline and amorphous regions

The as deposited films show two structural regions at the composition range studied). (First region is constituted of X-ray amorphous films, which can be identified in the range of Ti at. %= 37.31-54, Al at. %= 27.67-30.61 and C at. %= 22.53-36.92. The X-ray diffraction of some selected points within the amorphous range is shown in Fig. 4. The C/Ti ratio in the selected points varied from 0.42 to 0.97 while the Al concentration was kept between 24.73 and 26.08 at. %. From Figure 4, the 2 theta angle of the observed hump at C/Ti of 0.42 and 24.73 at.% of Al is $\sim 38^\circ$ with a FWHM of about 4.09° . (increasing the C/Ti from 0.42 to 0.97 the observed hump becomes more widespread with an average 2 theta angle of $\sim 38.5^\circ$, FWHM $\sim 12.9^\circ$).

In general, the increasing of Al concentration in the as-deposited Ti-Al-C films induces the formation of the X-ray amorphous however, by increasing the C/Ti ratio, the crystalline phase is more favorable, e.g., at $\text{Al} \leq 25$ at. % and $\text{C/Ti} > 0.75$.

Soldán et al. [31] reported that the deposition of Al into the Ti-C film at 500°C makes the formation of the X-ray amorphous phase visible at the Al concentration of 30-50 at. % and C/Ti of ~ 1 . Here, at relatively low substrate temperature (deposition without intentional heating), X-ray amorphous was observed at Al at. %= 27.67-30.6. The second region at this stage is constituted of a crystalline phase of Ti, Al and C in the range of Ti at. %= 36.74-60.55, Al at. %= 12.05-24.01 and C at. %= 22.73-47.69 (Figure 3). Figure 5 show the X-ray diffraction data of some points within this range at C/Ti ratio from 0.41 to 1.24 and Al concentration between 13.70 and 15.97 at.%. Within this range, it seems that the crystallinity is controlled by the carbon concentration as Ti is argued to be substitutional with Al.

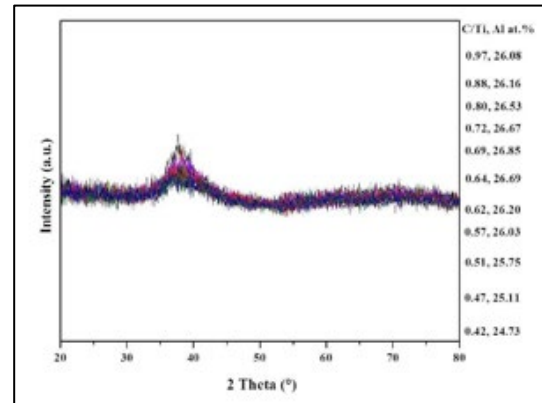


Figure 4: XRD results within the amorphous region

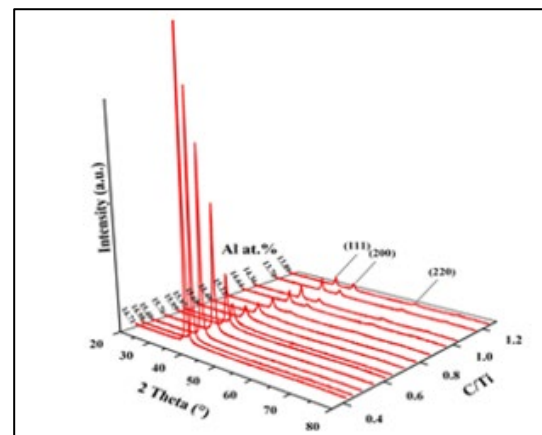


Figure 5: XRD results represent some effects of both C/Ti ratio and the Al concentration

That means the structural features of the crystalline film is influenced by the C/Ti ratio. At C/Ti of 0.41 and Al=14.71 at.%, film structure exhibits a single peak with 2 theta angle of $\sim 37^\circ$, FWHM $\sim 0.45^\circ$ and intensity of ~ 482 . By increasing C/Ti ratio of 1.24 at the Al content of 13.89 % at. (less than 1 at. %) the position and the intensity is reduced to $\sim 35.96^\circ$ and ~ 12.26 , respectively, however the FWHM is increased to $\sim 0.64^\circ$. This indicates larger lattice parameters as well as less ordered and smaller crystallites. Additional XRD peaks can be observed at 2 theta angle of ~ 42 and $\sim 60.5^\circ$ as the C/Ti ratio increased from 0.85 to 1.24 which may be contributing to the more random structure as compared with the low C/Ti ratio part $0.42 \leq \text{C/Ti} < 0.8$. Hence, the C/Ti ratio can play an active role on the lattice constant of TiC_x regardless of the Al concentration as well as its effects on the preferential orientation of the produced phase. Hence, increasing of C/Ti ratio for the same Al content as well as the increasing of the Al content for the same C/Ti ratio cause an increasing in the 2 theta angle indicating lattice expansion. This lattice parameters versus C/Ti

correlation is consistent with literature data of deposit TiCx [37,38]. However, the additional Al content further shifts the observed peak to higher 2 theta value (Figure 6), which results in more reduction in the unit cell as the Al atoms are smaller. Therefore, It is reasonable to assume that the crystalline phase observed at this stage can be contributed to the formation of TiC containing Al. The observation of a peak position at 2-theta $\geq 37^\circ$ for the TiC (111) plane (the standard 2-theta for (111) of TiC is 35.90° [39]) can be attributed to the lower C/Ti ratio and more Al atoms replace the Ti position in cubic unit cell. Wilhelmsson et al. [4] observed the formation of a metastable solid solution of Al in TiC at $T < 800^\circ\text{C}$ while sputtering the Ti-Al-C system from three elemental targets. Emmerlich et al. [40] reported the same observation for the deposited Ti-Si-C system at $T < 700^\circ\text{C}$ where a competitive TiCx growth with Si segregation to form twin boundaries or Si substitutional incorporated in TiCx structure were suggested. (epitaxial grown of Ti-Al-C and Ti-Si-C films on Al₂O₃ (0001) substrate was also observed in literatures [4, 40], which may explain the notice of a single XRD peak of the cubic (Ti, Al) C phase in some ternary regions).

4. Conclusion

Combinatorial magnetron sputtering of three different elemental powders was used to produce Ti-Al-C films with large composition gradient. This material library enabled to investigate through the phase formation after room temperature deposition by EDX and XRD. Two different regions within the area investigated was found, the first contains the (Ti, Al) C crystalline phase while the second includes the X-ray amorphous. A clear evidence is found to correlate with the lattice constant of the (Ti, Al) C with the Al concentration. By increasing the Al concentration in the crystalline phase, the lattice constant decreases slightly.

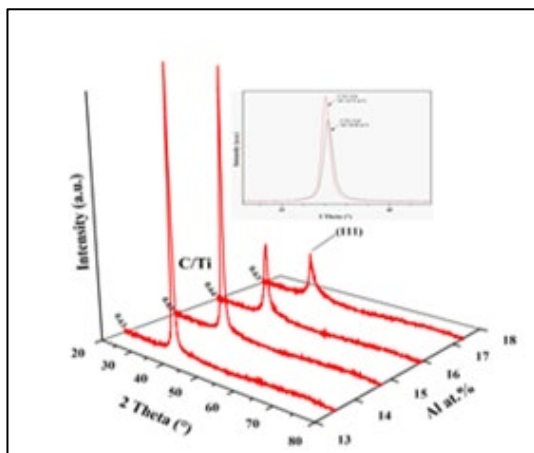


Figure 6: XRD results represent the effect of Al concentration with fixed C/Ti ratio on the crystallinity and peaks shift of (Ti, Al) C crystalline phase

References

- [1] O. Knotek, F. Löffler, I. Wolkers, Surf. Coat. Technol. 68/69, 176-180, 1994.
- [2] J.M. Lackner, W. Waldhauser, R. Ebner, J. Keckés, T. Schöberl, Surf. Coat. Technol. 177-178, 447-452, 2004.
- [3] M. Stueber, U. Albers, H. Leiste, S. Ulrich, H. Holleck, P.B. Barna, A. Kovacs, P. Hovsepian, I. Gee, Surf. Coat. Technol. 200, 6162-6171, 2006.
- [4] O. Wilhelmssona, J.-P. Palmquist, E. Lewina, J. Emmerlich, P. Eklund, P.O.Å. Perssonb, H. Högbergb, S. Li, R. Ahuja, O. Erikssonc, L. Hultman, U. Jansson, J. Cryst. Growth 291, 290-300, 2006.
- [5] M.W. Barsoum, T. El-Raghy, Am. Scient. 89, 334-343, 2001.
- [6] M.W. Barsoum, Prog. Solid St. Chem, 28, 201-281, 2000.
- [7] D. Music, J.M. Schneider, JOM 59 (2007) 60-64.
- [8] P. Eklund, M. Beckers, U. Jansson, H. Högberg, L. Hultman, Thin Solid Films 518, 1851-1878, 2010.
- [9] Z. Lin, M. Li, Y. Zhou, J. Mater. Sci. Technol. 23, 145-165, 2007.
- [10] J.D. Hettinger, S.E. Lofland, P. Finkel, T. Meehan, J. Palma, K. Harrell, S. Gupta, A. Ganguly, T. El-Raghy, M.W. Barsoum, Phys. Rev. B 72, 115120-115120-6, 2005.
- [11] M.W. Barsoum, T. El-Raghy, J. Am. Ceram. Soc. 79, 1953-1956, 1996.
- [12] N.V. Tzenov, M.W. Barsoum, J. Am. Ceram. Soc. 83, 825-832, 2000.
- [13] T. El-Raghy, A. Zavaliangos, M.W. Barsoum, S.R. Kalidindi, J. Am. Ceram. Soc. 80, 513-516, 1997.
- [14] Z. Sun, Y. Zhou, M. Li, Acta Mater. 49, 4347-4353, 2001.
- [15] A. Zhou, C. Wang, Y. Huang, Mater. Sci. Eng. A 352, 333-339, 2003.
- [16] J. Zhu, B. Mei, X. Xu, J. Liu, Mater. Lett. 58, 588-592, 2004.
- [17] L. Peng, Scr. Mater. 56, 729-732, 2007.
- [18] Y. Zou, Z.M. Sun, H. Hashimoto, S. Tada, Mater. Sci. Eng. A 473, 90-95, 2008.
- [19] V.G. -Brunet, T. Cabioc'h, P. Chartier, M. Jaouen, S. Dubois, J. Eur. Ceram. Soc. 29, 187-194, 2009.
- [20] O. Wilhelmsson, J.-P. Palmquist, T. Nzberg, U. Jansson, Appl. Phys. Lett. 85, 1066-1068, 2004.
- [21] C. Walter, C. Martinez, T. El-Raghy, J.M. Schneider, Steel Res. Int. 76, 225-228, 2005.
- [22] H. Högberg, L. Hultman, J. Emmerlich, T. Joelsson, P. Eklund, J.M. Molina-Aldareguia, J.-P. Palmquist, O. Wilhelmsson, U. Jansson, Surf. Coat. Technol. 193, 6-10, 2005.
- [23] W.Garkas, C. Leyens, A.F. Renteria, Adv. Mater. Res. 89-91, 208-213, 2010.

- [24] S. Riaz, H.M. Flower, D.R.F. West, *Mater. Sci. Technol.* 16, 984, 2000.
- [25] F.M. Samir, Y.L. Petitcorps, J. Etourneau, *J. Mater. Chem.* 7, 99, 1997.
- [26] W.H. Tian, M. Nemoto, *Intermet* 5, 237, 1996.
- [27] M. Witthaut, R. Cremer, A.v. Richthofen, D. Neuschütz, *J. Anal. Chem.* 361, 639, 1998.
- [28] W.-D. Munz, *J. Vac. Sci. Technol. A* 4, 2717, 1986.
- [29] A. Hörling, L. Hultman, M. Odén, J. Sjöle, L. Karlsson, *Surf. Coat. Technol.* 191, 384, 2005.
- [30] K.K. Al-Khazrajy, A.M.H. Al-Ghaban, M. N. A. Hussain, *Eng. & Tech. Journal*, Vol.33, Part (A), No.4, 2015.
- [31] J. Soldán, J. Musil, P. Zeman, *Plasma Processes Polym.*, 4, S6-S10, 2007.
- [32] R.S. Rawat, P. Leeb, T. White, Li Ying, S. Lee, *Surface and Coatings Technology*, vol.138, 159-165, 2001.
- [33] P. J. Martin, R. P. Netterfield, T. J. Kinder, *Surface and Coatings Technology*, vol. 49, pp. 239-243, 1991.
- [34] R. KuZel, Jr., R. cernf, V. Valvoda, M. Blomberg, M. Merisalo, S. Kadlec, *Thin Solid Films*, vol. 268, pp. 72-82, 1995.
- [35] U.C. Oh, J. Ho Je, *J. Appl. Phys.*, vol. 74, pp. 1692-1698, 1993.
- [36] N. Zarrinfar, P.H. Shipway, A.R. Kennedy, A. Saidi, *Scripta Materialia* 46 (2002) 121-126.
- [37] D.E. Wolfe, J. Singh, *Surf. Coat. Technol.* 124 (2000) 142-153.
- [38] E. Kusano, A. Satoh, M. Kitagawa, H. Nanto, A. Kinbara, *Thin Solid Films* 343-344 (1999) 254-256.
- [39] JCPDS card No. 32-1383.
- [40] J. Emmerlich, H. Högberg, S. Sasvári, P.O. Persson, L. Hultman, J.-P. Palmquist, U. Jansson, J.M. Molina-Aldareguia, Z. Czigány, *J. Appl. Phys.* 96 (2004) 4817-4826.

Author's biography

Assist. Prof. Dr. Ahmed M.H. Abdulkadhim Al-Ghaban Head of the Materials Eng. Department UOT Baghdad. BSc in Metallurgical Engineering, University of Technology. MSc in Metallurgical Engineering, University of Technology. PhD in materials Engineering/RWTH Aachen Germany. Many activities in the field of materials science and engineering.

